2025 IEEE Intelligent Vehicles Symposium (IV)
June 22-25, 2025. Cluj-Napoca, Romania

Generating Synthetic Deviation Maps for Prior-Enhanced Vectorized HD Map Construction

Haoming Xu[1,2], Yiyang Xiao[1,3], Wei Li[1,3*], *Member, IEEE*, Yu Hu[1,3], *Member, IEEE*

***Abstract*— High-definition (HD) maps are essential for autonomous driving, providing detailed and accurate environmental information. Recent advancements in online vectorized HD map construction have shown great promise, particularly methods that leverage existing maps as prior knowledge to improve performance. However, the robustness of these prior-enhanced methods under varying deviations between the priors and the real world remains a critical concern. This paper introduces a novel framework for generating synthetic maps, which allows for the controllable magnitude of diverse deviations, including geometric distortions, topological errors, and semantic inconsistencies, simulating real-world scenarios where prior maps may be outdated or inaccurate. Furthermore, lane group constraints are designed to avoid positional conflicts when map elements are modified. The synthesis method can overcome the time-consuming challenge of collecting real road changes. We demonstrate the utility of the synthetic deviation maps by incorporating them into the state-of-the-art prior-enhanced construction methods. The results reveal how different types and degrees of deviations affect the prediction accuracy, providing worthwhile insights into their robustness. Overall, this work contributes to a data augmentation and provides a valuable tool for developing more robust and reliable autonomous driving systems. The code is opensource and available at https://github.com/healenrens/Syn-D-maps.**

I. INTRODUCTION

Autonomous driving technologies encounter challenges that are difficult to address solely with sensors, including situations like heavy occlusions, unfavorable lighting, sharp curves in lanes, and severe weather. High-definition (HD) maps are crucial for the advancement of autonomous driving. With the centimeter-level accurate road geometry and rich semantic information, HD maps complement the sensor systems mounted on autonomous vehicles with beyond-line-of-sight (BLOS) data, thus enhancing their driving safety. However, the conventional pipeline for updating HD maps is subject to several inherent limitations. Their heavy reliance on professional surveying technologies and specialized equipment, coupled with mandatory reviews for data security, leads to high cost and prolonged update period. Consequently, existing surveying-based construction methods of HD map are unable to promptly reflect road changes, and insufficient to meet the real-time requirements of map data for autonomous vehicles [1]. In the following text, we will refer to the outputs from the above methods as offline maps.

This work was supported by Beijing Natural Science Foundation (L243008).
[1]The Research Center for Intelligent Computing Systems, Institute of Computing Technology, Beijing, 100190, China.
[2]Hangzhou Institute for Advanced Study, University of Chinese Academy of Sciences, Hangzhou, 310024, China.
[3]University of Chinese Academy of Sciences, Beijing, 100049, China.
*Corresponding author. Email: liwei2019@ict.ac.cn.

As an alternative to the conventional pipeline, online vectorized HD map construction [2]–[6] has been introduced to ensure the freshness of map data in highly dynamic and complex road network environments. This construction task typically takes surrounding images or LiDAR points as input, then projects features into bird's-eye view (BEV), and finally predicts a vectorized local semantic map. Nevertheless, online HD map construction still exhibits a considerable gap in accuracy and mapping scale compared to surveying-based techniques. To narrow the gap, current researches [7]–[13] attempt to leverage available offline maps as prior knowledge to enhance online map prediction capabilities. P-MapNet [8] designs a pipeline to incorporate both standard-definition (SD) map and HD map priors into online map generators. The SD map priors features, represented in the BEV space, are fused with sensor features using an attention mechanism, while HD map priors are injected through a masked autoencoder for output refinement. Zhang *et al.* [10] focus on leveraging offline SD maps as priors and investigate their prototypical representations, demonstrating that the prior information can speed up the convergence of online mapping task.

Unfortunately, if there are errors or large deviations in the offline maps serving as prior knowledge, it can severely impact the aforementioned existing methods. MapEX [12] notes this problem and encodes offline-map elements into query tokens as a supplement to classic learned queries. However, it limits the discussion to only three types of existing maps (minimalist, noisy and outdated), whereas studies on road changes in real-world reveal that offline maps exhibit more diverse alterations [14]–[16]. Thus, for research on prior-enhanced vectorized HD map construction, there is a critical demand for offline-map datasets that reflect real-world road changes and encompass a comprehensive range of alteration types.

According to the research spanning more than five years on German highways [15], almost 200 major road changes, including lane markings, guardrails, and complete reconstruction, resulting in more than 41% of offline maps becoming outdated. Due to the considerable time cost involved in collecting such datasets, generating synthetic map deviations is becoming a viable alternative. Existing methods for map synthesis [12], [16], [17] do not fully cover the range of real-world road changes and neglect the positional conflicts that may arise from the addition or removal of instances. Furthermore, these current synthetic approaches also lack the ability to quantify and control the degree of deviation. Therefore, in order to better reflect the issues that exist in

2025 IEEE Intelligent Vehicles Symposium (IV) | 979-8-3315-3803-3/25/$31.00 ©2025 IEEE | DOI: 10.1109/IV64158.2025.11097394

TABLE I
SUMMARY OF MODIFICATIONS AND OBJECTS IN SYNTHETIC MAP DEVIATION METHODS

Synthetic Modification	MapModEX [12]	TbV [16]	Bateman *et al.* [17]	Ours-SynD
Removal/Delete	Map elements	Lane marking, crosswalk	Polyline features	Map elements, lane elements within a lane group
Addition/Insert		Bike lane, crosswalk		
Translation/Shift	Global map, crosswalk	-	Global map	Global map, lane group
Rotation	Global map	-	Global map	Global map
Warping	Global map	-	Perlin warp	Any selected lane elements
Noise	Point coordinates	-	Control point, feature location	Point coordinates, lane elements
Change	-	Lane boundary dash-solid, lane marking color	Types of polyline features	Types of map points
Group	-	-	-	Lane elements (boundaries, lanes, dividers)
Open source	✓	✗	✗	✓

offline maps, and to mitigate the sim-to-real gap, we propose a method for synthesizing map deviations with controllable degree, which is abbreviated as SynD in the following text. By introducing the concept of lane groups, we fully consider the positional consistency of adjacent map elements after changes. SynD is designed to be compatible with widely used autonomous driving datasets, such as nuScenes [18] and Argoverse [19], [20], simulating the map deviations induced by outdated or surveying errors. This will be beneficial in alleviating data scarcity issues during training in relevant research, as well improve the performance and generalization capabilities of prior-enhanced algorithms in scenarios involving road reconstructions.

Overall, the main contributions of this paper are threefold.

- A lane group partitioning method based on Principal Component Analysis (PCA) is proposed. Compared to single straight-line lane models, this approach can describe the main direction of curved lanes. Based on this, lanes with the consistent direction are unified into a group, avoiding positional conflicts of adjacent instances when modifying map elements.
- A controllable deviation synthesis method for offline maps is designed. We divide the offline HD map into geometric, topological, and semantic layers, and parameterize offset operations for each layer, thereby enabling flexible adjustment of the deviation magnitude to simulate varying map errors.
- We conducted adequate experiments on existing prior-enhanced vectorized HD map construction methods using the synthesized deviation maps. Results demonstrate that the presence of errors in prior offline maps pose a significant challenge to the robustness of these methods, highlighting the necessity to explore the fault tolerance of prior information.

II. RELATED WORK

A. Online Vectorized HD Map Construction

With recent advancements in machine learning, online vectorized HD map construction offers an alternative to labor-intensive traditional methods that involve expensive surveying equipment. Early methods first construct rasterized maps with semantic segmentation and then generate vectorized maps through post-processing [2]. VectorMapNet [21] and MapTR [3] directly predict the vectorized map elements which are represented as polylines through Transformer-based models. As an enhanced version, MapTRv2 [4] proposes a decoupled self-attention mechanism in the inter-instance and intra-instance dimensions, significantly reducing memory consumption. Other methods model the instances with geometric properties as polynomial curves [6], [22], [23] instead of polylines. This benefits the improvement trend by employing shape and geometry priors of lanes and pedestrian crossings [24], [25].

B. Prior-Enhanced HD Map Construction

Leveraging offline maps as prior knowledge to help the online vectorized HD map construction can alleviate negative impacts such as occlusion by on-road objects, leading to increased prediction accuracy. Through the interpolation and concatenation of SD map features with BEV image features, Zhang *et al.* [10] make use of SD maps as priors to speed up convergence and boost performance. Yang *et al.* [11] make the algorithm learn structural prior information by using SD map features as the key and value, and the feature map from images as the query to implement cross-attention. P-MapNet [8] shares a similar approach in exploiting SD map priors, beyond this, it also employs a pre-trained HDmap prior module for refinement. MapEX [12] introduces a novel design to utilize existing HD maps as guidance, through the implementation of a map query encoding module and a pre-attribution of predictions. Apart from relying on offline maps for assistance, NMP [7] and HRMapNet [13] enhance the vectorized map perception with historical maps obtained from vehicles that have previously traversed the same region. HRMapNet [13] designs an aggregation module and a query initialization module, that exploit the historical rasterized map in terms of BEV features and map element queries respectively. As a inclusive framework, PriorDrive [9] proposes a unified vector encoder to learn the prior distribution from three types mentioned above, including SD maps, outdated HD maps and online historical prediction maps. While these existing works have demonstrated the effectiveness of prior-enhanced approaches, they have not sufficiently discussed

TABLE II
CLASSIFICATION OF MAP CHANGE/ERRORS IN REAL WORLD AND CORRESPONDING SYNTHETIC MODIFICATIONS

Layer	Change/Error Type	Synthetic Modification
Geometric	Localization error when generating offline maps	Map global translation
		Map global rotation
	Sensor noise	Gaussian noise
Semantic	Incorrect types of objects	Label conversion
	Missing semantic label	Label deletion
Topological (caused by reconstruction, temporary diversions, etc.)	Lane number change	Lane addition
		Lane reduction
	Lane width change	Lane widening
		Lane narrowing
	Lane Separation Removal	Lane dividers deletion
	Road closure	Lane group deletion
	Road Distortion	Bézier warping

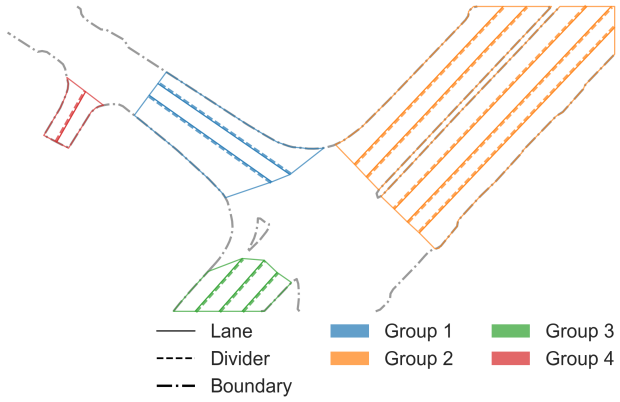

Fig. 1. Illustration of lane grouping concept.

whether such methods maintain robustness under different degrees of biased prior information.

C. Synthetic Map Deviation Technique

Because monitoring real-world road changes is a time-consuming process, typically spanning years, some existing research addresses this limitation by generating synthetic map discrepancies that emulate situations caused by reconstruction, traffic management, temporary diversions, and road degradation. Table I details the modifications and objects provided by existing methods for synthetic map deviation. MapModEX [12] is a standalone library designed to take true HD maps from nuScenes files as input and synthetically generate imprecise maps. It supports a relatively complete range of operations, but lacks consideration of changing the semantic types of map elements. TbV dataset [16] has a supplementary work of generating realistic-appearing synthetic maps, aimed at providing fake negatives for training. Its primary focus lies on the modification of lane geometry and crosswalks, with no inclusion of positional changes like shift and rotation. Bateman *et al.* [17] classified the types of synthetic map prior perturbation into discrete and continuous, warping mutations. Regrettably, none of the aforementioned works considered potential positional conflicts among map elements caused by modifications, nor whether the coordinates of other related instances need to be adjusted after lane removal or addition.

III. METHODOLOGY

Based on the preceding analysis of synthetic maps requirements, we propose a systematic framework for generating maps with controllable variations. Our framework categorizes map changes into geometric, semantic, and topological layers, with supported change and error types as illustrated in Table II. The first contribution of this work is a PCA-based grouping method for lane elements. This method facilitates topological modifications performed at the group level, thereby ensuring that the synthetic distortions more faithfully reflect realistic deviations. The implementation of this aspect is discussed in Section III-A. Additionally, to quantify and control the distortion magnitude, we define a set of novel metrics for HD map alterations in Section III-B. The third innovation, in the geometric layer, is the introduction of a warping method based on cubic Bézier curves, as detailed in Section III-C.

A. Lane Grouping via Direction-Based Clustering

Real-world road variations, resulting from reconstruction, or road maintenance, generally impact multiple lanes within a defined area. During the process of generating synthetic maps, using individual lanes as modification units often fails to maintain consistency and rationality. Therefore, we introduce the concept of "Lane Group", which organizes lanes with similar geometric and topological characteristics, along with their associated map elements (such as lane dividers and road boundaries), into a unified minimal modification unit. This enables a more effective preservation of the original topological structure in the synthesized map. Even for current HD map datasets, there is no dataset that can directly provide the labels for the varying range of lane groups.

We define a lane group as a collection of lanes sharing similar geometric features and topological relationships, as shown in Fig. 1. While this grouping operation is intuitively simple from a human visual perspective, the coordinate-based point collection storage format of offline maps presents implementation challenges. While learning-based approaches might effectively address this issue given sufficient data, the current scarcity of annotated data renders them impractical. Therefore, we develop our approach from fundamental principles, considering that when lanes undergo changes, they typically influence other lanes with similar forward directions (or closely opposite directions) and spatial proximity.

Based on the aforementioned observations, we define the complete set of lanes $L = \{L_1, L_2, ..., L_n\}$ in a map. For each individual lane L_i, we can compute its principal direction vector $\mathbf{D_i^P}$ using Principal Component Analysis (PCA). Considering that the geometry of most lanes can be approximated as rectangular shapes. So we calculate minimum bounding rectangle of each lanes and use their long edge direction $\mathbf{D_i^r}$ approximately representing the primary

direction of lane. Finally, We define the direction vector set $D = \{\mathbf{D_1}, ..., \mathbf{D_n}\}$ of a lane using the following equation:

$$\mathbf{D_i} = \frac{\alpha \mathbf{D_i^p} + \beta \mathbf{D_i^r}}{\|\alpha \mathbf{D_i^p} + \beta \mathbf{D_i^r}\|_2} \tag{1}$$

where:

$$\alpha^2 + \beta^2 = 1 \tag{2}$$

Beyond directional constraints, distance constraints are equally crucial to ensure spatial consistency and realistic lane group formations. Our method is using the mutual distances $S_{ij} = \|\mathbf{C_i} - \mathbf{C_j}\|_2$. Where $\mathbf{C_i}$ and $\mathbf{C_j}$ represent geometric centers of points which compose different lanes in the set L. It performs well due to its ability to adapt to dynamic lane numbers. However, direct iterative grouping will make the results dependent on lane data storage order, or require a lot of processing time. To address this issue, we implement a Union-Find data structure in our grouping method, as detailed in Algorithm 1.

B. Metrics for Controllable Deviation Synthesis

After establishing the lane grouping mechanism, another crucial aspect of synthetic map generation is controlling and evaluating the metrics of map changes. This needs a set of robust and quantifiable metrics, as they will significantly influences the evaluation of downstream tasks. Considering the diverse characteristics of road changes, we approach this evaluation from two perspectives: geometric metrics for the geometric layer and instance metrics for the semantic and topological layers.

1) Geometric Metrics: For geometric changes of point sets that comprise instances, we begin by considering the proportion of changed points within a single instance. Given that the ith instance has N_i^t total points, among which N_i^w points exhibit significant changes (above threshold R), we define the change degree E_i^R for a single instance as:

$$E_i^R = \frac{N_i^w}{N_i^t} \tag{3}$$

where threshold R can take different values to represent three levels (R_h:high, R_m:medium, R_l:low). Because the modifications of rotation, translation, and noise addition all induce positional changes, we select 1.5m, 1.0m, and 0.5m as corresponding thresholds, consistent with the evaluation standards of downstream tasks. After building upon individual instance change degrees, we further define two global metric indicators: Discrete Change Degree ED_τ^R and Continuous Change Degree EC^R.

The Discrete Change Degree reflects the proportion of instances experiencing noticeable changes with another given threshold τ:

$$ED_\tau^R = \frac{\sum_{i=1}^{N_T} N_i^R}{N_T} \tag{4}$$

where:

$$N_i^R = \begin{cases} 1, & \text{if } E_i^R > \tau \\ 0, & \text{if } E_i^R \leq \tau \end{cases} \tag{5}$$

Algorithm 1: Lane Grouping Algorithm

Input: $L = \{L_1, ..., L_n\}$, $D = \{\mathbf{D_1}, ..., \mathbf{D_n}\}$[1], $S = \{S_{11}, ..., S_{nn}\}$[1], threshold θ_d and θ_a
Output: Grouping result $G = \{G_1, ..., G_k\}$

Initialize global:$parent[i] = i$, $i \in N, 1 \leq i \leq n$
Initialize global:$rank = \mathbf{1_{1xn}}$
Function *Find(x)*[1] **:**
  if *parent[x] = x* **then**
    return x
  else
    parent[x] ← Find(parent[x])
    return parent[x]
  end
end
Function *Union(x, y)*[1] **:**
  root_x ← Find(x) root_y ← Find(y)
  if *root_x != root_y* **then**
    if *rank[root_x] >rank[root_y]* **then**
      parent[root_y] ← root_x
    else if *rank[root_x] <rank[root_y]* **then**
      parent[root_x] ← root_y
    else
      parent[root_y] ← root_x
      rank[root_x] ← rank[root_x] + 1
    end
  end
end
for $i \leftarrow 1$ **to** n **do**
  for $j \leftarrow i + 1$ **to** n **do**
    if $\arccos(\mathbf{D_i} \cdot \mathbf{D_j}) < \theta_a$ *and* $S_{ij} < \theta_d$ **then**
      Union(i,j)
    end
  end
end
Create empty dictionary $G \leftarrow \{\}$
for $i \leftarrow 1$ **to** n **do**
  $g \leftarrow$ Find(i)
  if $g \notin G$ **then**
    $G[g] \leftarrow \{\}$
  $G[g] \leftarrow G[g] \cup \{L_i\}$ `// Add lane to group`
end
return G

[1]**Note:** For each lane, its direction vector $\mathbf{D_i}$ and mutual distances $\mathbf{S_{ij}}$ is computed as aforementioned. Find and Union are standard disjoint-set [26] operations with path compression and rank optimizations.

Here, N_i^R is a binary variable that indicates whether the change degree $E_i^{R_h}$ of a single instance exceeds the threshold τ, and NT denotes the total number of instances in a map.

The Continuous Change Degree directly accumulates the change degree E_i^R of all instances, as $EC^R = \sum_{i=1}^{N_T} E_i^R$. It provides a finer-grained global assessment.

We propose both continuous and discrete global metrics because different types of changes induce disparate effects on instances and points, making certain indicators more suitable for specific changes. By adjusting thresholds R and τ, we can flexibly control the sensitivity of change detection to accommodate various downstream task evaluation standards.

2) Semantic and Topological Metrics: For semantic and topological layer changes, which build upon geometric changes and reflect higher-level modifications, considering point-wise changes would unnecessarily complicate the met-

rics. Inspired by the previous work [14], we focus on the overall proportion of instance changes instead of individual variations. Modifications in topological and semantic layers can be categorized into three types: addition, removal, and changes in geometric layer and semantic layer. Any changes in these two layers can be decomposed into the three types. Based on this categorization, we define the Instance Metric (IM) as follows:

$$IM = \frac{|Es_{added}| + |Es_{removed}| + |Es_{modified}|}{|Es_{total}|} \quad (6)$$

Es_{added} and $Es_{removed}$ indicate how many instances have been added and removed respectively. $Es_{modified}$ indicate how many times original instances are changed in geometric layer and semantic layer, Es_{total} denotes the total number of instances in the map. While this metric effectively describes semantic and topological changes, directly applying it as a standard in the synthetic map framework is challenging because a single change may involve multiple operations. For a map, directly using IM as a target complicates the automatic allocation of operation quantities, as the relationship between operations and changes is not always one-to-one.

Therefore, for semantic and topological layer changes, we use lane groups or lanes as modification units and target the number of changed lane groups or lanes. Since achieving a specific change target within a given area is not always guaranteed, IM serves as a posterior indicator to evaluate the actual extent of changes. Notably, we assign equal importance to different types of instances, while different types of modifications affect instance proportions differently. This means that IM value is not necessarily equal between different types of changes or errors, though they remain comparable within the same type, as demonstrated in subsequent experiments. This combined approach simplifies the control of changes during map synthesis while maintaining the precision of instance metrics.

3) Implement Detail of Controllable Deviation: As mentioned aforementioned, in the geometric layer, we directly use geometric metrics as control parameters. For example, we employ ED metrics for global rotation operations. We utilize a binary search algorithm starting from 90 to iteratively solve for the rotation angle until the ED difference between the modified map and the target ED falls below a specified threshold, with a maximum iteration limit of 1000. For gaussian noise, we adopt EC metrics as the target measure, but instead of modifying all instances, we select instances based on their point count and then randomly choose points within these instances to meet the target EC quantity for noise addition.

In semantic and topological layer modifications, we use modified lane ratio or lane group ratio as control parameters. As for lane number changes, we select group ratio which means the percentage of groups will be modified. In the case of addition deviation, we locate lanes on both sides of the lane group and shift them outward by the average lane width of the group (associated road boundaries are shifted accordingly), then add new lanes and lane dividers at the original positions. Similarly, for reduction deviation, which also belongs to number changes, we first select target lane groups and then randomly choose lanes within the group for removal, replacing the associated dividers with boundaries, and adding additional connecting lines where boundaries become disconnected due to the removal.

C. Bézier Curve-based Warping

At the geometric deformation layer, we adopt cubic Bézier curves as our warping tool.It will ensure that deformed map elements maintain their previous geometric and topological relationships and we can precisely control both the degree and direction of deformation while maintaining consistency within and between lane groups.

After balancing computational complexity and effectiveness, we implement warping using cubic Bézier curves. For any line segment element in the map, we define its start point as P_0 and end point as P_3. Given a weight parameter w, we construct four control points for the cubic Bézier curve:

$$\begin{aligned} P_1 &= P_0 + \frac{1}{3}(P_3 - P_0) + w\|P_3 - P_0\|\tilde{\mathbf{n}} \\ P_2 &= P_0 + \frac{2}{3}(P_3 - P_0) + w\|P_3 - P_0\|\tilde{\mathbf{n}} \end{aligned} \quad (7)$$

where $\tilde{\mathbf{n}}$ is the unit normal vector of the line segment, and w is the deformation weight coefficient. Note that non-uniform control point selection methods can also be applied. Based on these control points, any point $P(t_i)$ on the curve can be calculated through the following parametric equation:

$$P(t_i) = (1-t_i)^3 P_0 + 3t_i(1-t_i)^2 P_1 + 3t_i^2(1-t_i)P_2 + t_i^3 P_3$$
$$t_i \in [0, 1] \quad (8)$$

To ensure realistic deformation while maintaining appropriate point density, we employ an adaptive sampling strategy. For a line segment of length L, we determine the number of sampling points N as:

$$N = \max(\lceil \frac{L}{d_s} \rceil, N_{min}) \quad (9)$$

where d_s is the desired sampling interval, and N_{min} is the minimum number of sampling points required for curve smoothness. The sampling points are generated using $t_i = \frac{i}{N-1}$, and $i = 0, 1, \ldots, N-1$. This adaptive sampling and mapping strategy guarantees that deformed elements retain an appropriate point density while preserving their inherent geometric characteristics.

This design allows the warping operation to be applied with precision, enabling fine-grained control over the degree and direction of deformation.

IV. EXPERIMENTS AND ANALYSIS

A. Dataset and Metrics

Our SynD framework exhibits broad compatibility with various data structures. We choose nuScenes as our dataset, which is one of the most widely used datasets for HD maps construction task. Following standard evaluation protocols, we segment offline HD maps into 30×60 meter sections.

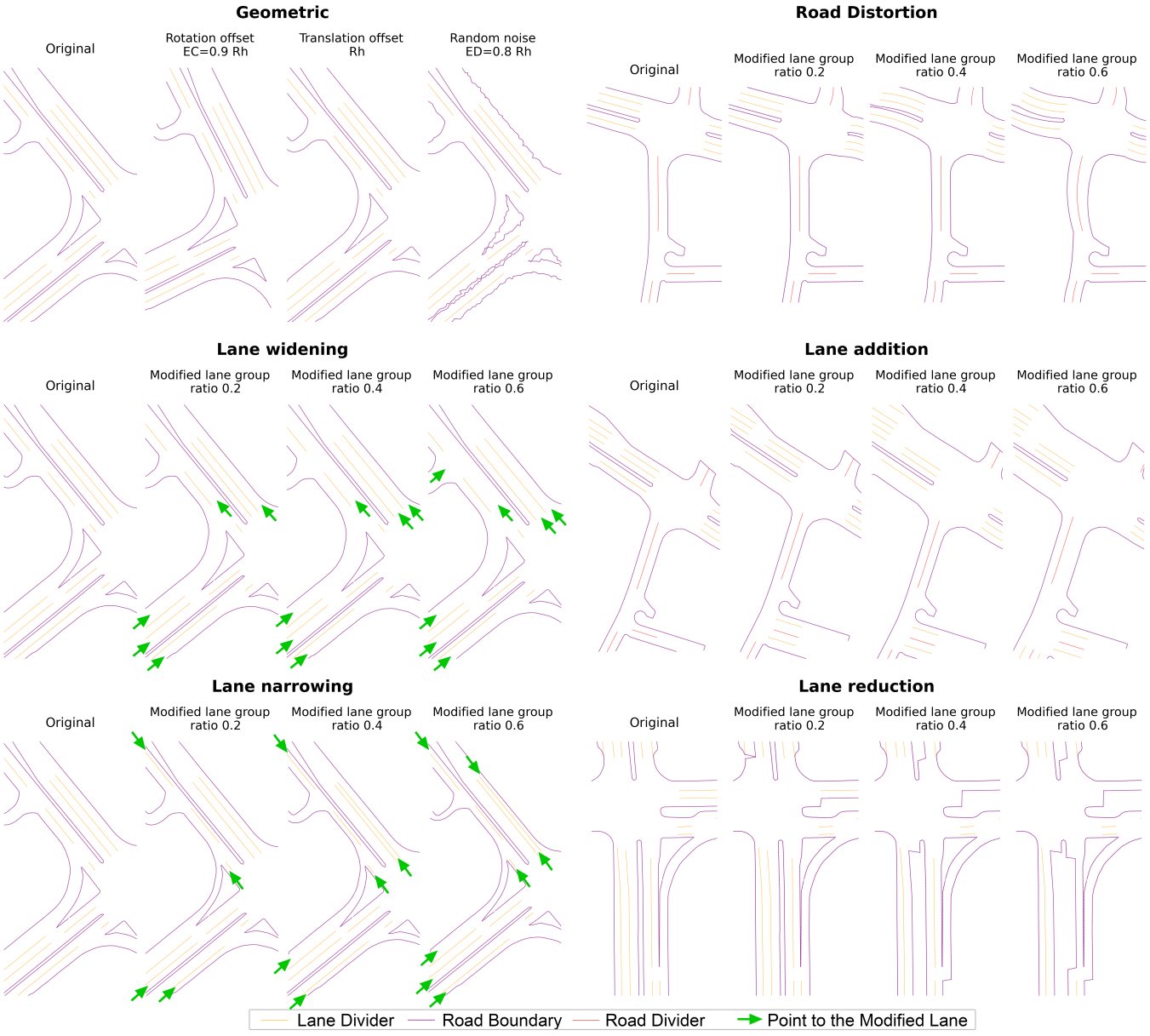

Fig. 2. Illustration of varying synthetic modifications with different magnitudes.

For geometric transformations, we use $R_h = 1.5$ for rotation and noisy. And rotation follow the ED metric with a $\tau = 0.5$ and difference below 0.01. The noisy in our experiments is generated using the R_h as the baseline, with a mean of half the R_h and a standard deviation of 0.15 times of the R_h. The effects of different modifications are shown in Fig. 2, where we use larger parameters for geometric changes to enhance visualization clarity.

B. Experimental Design

To evaluate how different types and degrees of prior deviation affect online map construction methods, we incorporated our synthetic maps into existing prior-enhanced approaches [7]–[13]. Because of open-source restrictions, we selected HRMapNet [13] for assessing the robustness. The architecture and weights of HRMapNet were preserved. The only adjustment made was replacing the prior input during inference with biased synthetic maps generated by SynD. We also applied the same replacement strategy to P-MapNet [8]. Contrary to intuition, the quantitative metrics (mIoU and mAP) derive from P-MapNet, while degraded by the perturbation, did not exhibit a clear correlation trend with the variations in the degree of deviation. Instead, the metrics exhibited oscillatory patterns. The primary reason may be attributed to the diversity of methods for generating SD maps, while the OpenStreetMap data utilized by P-MapNet lacks implementation details, potentially leading to data alignment issues. Given these considerations, our

TABLE III

PERFORMANCE COMPARISON OF GEOMETRIC AND SEMANTIC MAP MODIFICATIONS

Layer	Modification Type	Control Metrics	HRMapNet				ΔmAP	IM
			AP_{div}	AP_{ped}	AP_{bou}	mAP		
Baseline (No modification in prior maps)			86.2	81.0	83.6	83.6	-	-
Geometric	Map global translation	$R_l = 0.5m$	48.97	76.96	57.19	61.04	$-22.6\,\%\downarrow$	-
		$R_m = 1.0m$	45.42	75.39	51.08	57.30	$-26.3\,\%\downarrow$	-
		$R_h = 1.5m$	46.00	74.12	52.03	57.38	$-26.2\,\%\downarrow$	-
	Map global rotation	ED = 0.2	52.85	77.56	59.31	63.24	$-20.4\,\%\downarrow$	-
		ED = 0.4	49.59	77.15	57.24	61.33	$-22.3\,\%\downarrow$	-
		ED = 0.6	48.80	76.64	54.50	59.98	$-23.6\,\%\downarrow$	-
	Gaussian noise	EC = 0.2	72.32	78.35	75.97	75.54	$-8.1\,\%\downarrow$	-
		EC = 0.4	69.69	78.32	73.32	73.78	$-9.8\,\%\downarrow$	-
		EC = 0.6	66.35	78.14	70.71	71.73	$-11.9\,\%\downarrow$	-
Semantic	Label conversion	Ratio = 0.2	56.58	77.85	68.62	67.69	$-15.9\,\%\downarrow$	0.58
		Ratio = 0.4	55.01	77.63	67.45	66.70	$-16.9\,\%\downarrow$	0.63
		Ratio = 0.6	51.04	77.30	65.71	64.68	$-18.9\,\%\downarrow$	0.78
	Label deletion	Ratio = 0.2	66.12	77.93	77.66	73.91	$-9.7\,\%\downarrow$	0.30
		Ratio = 0.4	64.05	77.82	77.68	73.18	$-10.4\,\%\downarrow$	0.41
		Ratio = 0.6	60.50	77.31	77.66	71.82	$-11.8\,\%\downarrow$	0.57

subsequent analyses primarily focus on HRMapNet as the baseline.

For geometric changes, we use R_h and test with EC or ED values of 0.2, 0.4, and 0.6. For semantic and topological changes, we employ the same three values as modification ratios.

C. Results and Analysis

We conducted experiments using the previously described parameters. Overall, different types of modifications showed varying impacts on model performance while maintaining consistency with posterior metrics. As shown in Table III, for geometric changes, global rotation and translation operations strongly affected model performance, with relatively little sensitivity to intensity variations. We attribute this to the fact that once significant displacement occurs, models tend to rely more heavily on sensor information for mapping, making subsequent intensity changes less significant.

For semantic changes, the models maintained good robustness, with accuracy degradation showing a strong positive correlation with modification ratios. We believe that As illustrated in Table IV, in semantic layer modifications, we observed phenomena similar to global changes during addition operations. This similarity can be attributed to our use of displacement methods to adjust other instances during lane addition operations to maintain map authenticity, which shares characteristics with global translation. For deletion and shape modification operations, we observed that model performance demonstrated clear positive correlations with both modification ratios and IM metrics.

These findings reveal that prior map deviations critically undermine the robustness of existing prior-enhanced algorithms. The observed performance degradation patterns emphasize the urgent need for enhanced data augmentation strategies during training. Furthermore, the distinct responses to different modification types provide foundational insights for developing fault-tolerant prior integration mechanisms. This systematic analysis validates the practical value of our proposed synthetic framework in diagnosing and improving map prior utilization.

V. CONCLUSION

This paper presents a novel method for generating synthetic deviation maps, which are designed to simulate the differences between offline maps and actual road alignments. Previous synthetic approaches did not consider potential overlaps between adjacent map elements caused by artificial modifications, thus exhibiting a sim-to-real gap compared to the outdated maps caused by road reconstructions in real world. We address this problem by proposing a PCA-based lane group concept. In addition, as the proposed SynD method permits manipulation of both the type and degree of map deviations, this facilitates a more effective evaluation of the robustness of online map construction methods and establishes a data substrate for future research on the fault tolerance. Furthermore, the generated deviation maps can be used to augment training data, leading to improvements in the robustness of prior-enhanced HD map construction.

In our future work, we will explore the synthetic framework using generative methods based on neural networks, for example Generative Adversarial Networks (GANs) and diffusion models. This will enable the more streamlined batch generation of numerous road changes that closely resemble those in real-world settings.

REFERENCES

[1] X. Tang, K. Jiang, M. Yang, Z. Liu, P. Jia, B. Wijaya, T. Wen, L. Cui, and D. Yang, "High-definition maps construction based on visual sensor: A comprehensive survey," *IEEE Transactions on Intelligent Vehicles*, 2023.

[2] Q. Li, Y. Wang, Y. Wang, and H. Zhao, "Hdmapnet: An online hd map construction and evaluation framework," in *2022 International Conference on Robotics and Automation (ICRA)*, 2022, pp. 4628–4634.

[3] B. Liao, S. Chen, X. Wang, T. Cheng, Q. Zhang, W. Liu, and C. Huang, "Maptr: Structured modeling and learning for online vectorized hd map construction," in *The Eleventh International Conference on Learning Representations*, 2023.

[4] B. Liao, S. Chen, Y. Zhang, B. Jiang, Q. Zhang, W. Liu, C. Huang, and X. Wang, "Maptrv2: An end-to-end framework for online vectorized hd map construction," *International Journal of Computer Vision*, pp. 1–23, 2024.

TABLE IV

PERFORMANCE COMPARISON OF TOPOLOGICAL MAP MODIFICATIONS

Deviation	Modification Type	Modified Ratio	HRMapNet				ΔmAP	IM
			AP_{div}	AP_{ped}	AP_{bou}	mAP		
Baseline (No modification in prior maps)			86.2	81.0	83.6	83.6	-	-
Addition	Lane addition	0.2	63.08	75.67	60.97	66.57	−17.0 %↓	0.70
		0.4	62.61	75.66	61.58	66.62	−17.0 %↓	0.84
		0.6	62.03	75.74	61.81	66.53	−17.1 %↓	0.93
Deletion	Lane reduction	0.2	69.68	75.80	74.93	74.37	−9.2 %↓	0.10
		0.4	67.90	78.23	73.68	73.27	−10.3 %↓	0.12
		0.6	66.25	78.23	72.19	72.22	−11.4 %↓	0.14
	Lane dividers deletion	0.2	71.38	78.29	77.89	75.85	−7.8 %↓	0.28
		0.4	70.37	78.19	77.84	75.59	−8.0 %↓	0.36
		0.6	70.11	78.14	77.86	75.37	−8.2 %↓	0.43
	Lane group deletion	0.2	69.35	77.19	74.94	73.83	−9.8 %↓	0.37
		0.4	67.41	76.84	73.80	72.69	−10.9 %↓	0.52
		0.6	65.55	76.45	72.09	71.36	−12.2 %↓	0.67
Shape modification	Lane widening	0.2	61.15	78.01	66.02	68.39	−15.2 %↓	0.91
		0.4	59.53	77.88	63.33	66.91	−16.7 %↓	1.34
		0.6	56.09	77.33	59.27	64.23	−19.4 %↓	1.91
	Lane narrowing	0.2	61.15	77.84	67.42	68.80	−14.8 %↓	0.91
		0.4	59.56	77.58	65.33	67.49	−16.1 %↓	1.34
		0.6	57.35	77.49	62.15	65.56	−18.0 %↓	1.91
	Bézier warping	0.2	71.33	78.74	76.13	75.40	−8.2 %↓	0.53
		0.4	70.58	78.74	75.63	74.98	−8.6 %↓	0.70
		0.6	69.40	78.46	74.85	74.24	−9.4 %↓	0.92

[5] Z. Liu, X. Zhang, G. Liu, J. Zhao, and N. Xu, "Leveraging enhanced queries of point sets for vectorized map construction," in *European Conference on Computer Vision*. Springer, 2025, pp. 461–477.

[6] L. Qiao, W. Ding, X. Qiu, and C. Zhang, "End-to-end vectorized hd-map construction with piecewise bezier curve," in *Proceedings of the IEEE/CVF Conference on Computer Vision and Pattern Recognition*, 2023, pp. 13 218–13 228.

[7] X. Xiong, Y. Liu, T. Yuan, Y. Wang, Y. Wang, and H. Zhao, "Neural map prior for autonomous driving," in *Proceedings of the IEEE/CVF Conference on Computer Vision and Pattern Recognition*, 2023, pp. 17 535–17 544.

[8] Z. Jiang, Z. Zhu, P. Li, H.-a. Gao, T. Yuan, Y. Shi, H. Zhao, and H. Zhao, "P-mapnet: Far-seeing map generator enhanced by both sdmap and hdmap priors," *IEEE Robotics and Automation Letters*, vol. 9, no. 10, pp. 8539–8546, 2024.

[9] S. Zeng, X. Chang, X. Liu, Z. Pan, and X. Wei, "Driving with prior maps: Unified vector prior encoding for autonomous vehicle mapping," *arXiv preprint arXiv:2409.05352*, 2024.

[10] H. Zhang, D. Paz, Y. Guo, A. Das, X. Huang, K. Haug, H. I. Christensen, and L. Ren, "Enhancing online road network perception and reasoning with standard definition maps," in *2024 IEEE/RSJ International Conference on Intelligent Robots and Systems (IROS)*, 2024, pp. 1086–1093.

[11] Z. Yang, M. Liu, J. Xie, Y. Zhang, C. Shen, W. Shao, J. Jiao, T. Xing, R. Hu, and P. Xu, "Mapvision: Cvpr 2024 autonomous grand challenge mapless driving tech report," *arXiv preprint arXiv:2406.10125*, 2024.

[12] R. Sun, L. Yang, D. Lingrand, and F. Precioso, "Mind the map! accounting for existing map information when estimating online hdmaps from sensor," *arXiv preprint arXiv:2311.10517*, 2024.

[13] X. Zhang, G. Liu, Z. Liu, N. Xu, Y. Liu, and J. Zhao, "Enhancing vectorized map perception with historical rasterized maps," in *European Conference on Computer Vision*. Springer, 2025, pp. 422–439.

[14] C. Plachetka, N. Maier, J. Fricke, J.-A. Termöhlen, and T. Fingscheidt, "Terminology and analysis of map deviations in urban domains: Towards dependability for hd maps in automated vehicles," in *2020 IEEE Intelligent Vehicles Symposium (IV)*. IEEE, 2020, pp. 63–70.

[15] J.-H. Pauls, T. Strauss, C. Hasberg, M. Lauer, and C. Stiller, "Can we trust our maps? an evaluation of road changes and a dataset for map validation," in *2018 21st International Conference on Intelligent Transportation Systems (ITSC)*. IEEE, 2018, pp. 2639–2644.

[16] J. Lambert and J. Hays, "Trust, but verify: Cross-modality fusion for HD map change detection," in *Thirty-fifth Conference on Neural Information Processing Systems Datasets and Benchmarks Track (Round 2)*, 2021.

[17] S. M. Bateman, N. Xu, H. C. Zhao, Y. Ben Shalom, V. Gong, G. Long, and W. Maddern, "Exploring real world map change generalization of prior-informed hd map prediction models," in *Proceedings of the IEEE/CVF Conference on Computer Vision and Pattern Recognition (CVPR) Workshops*, June 2024, pp. 4568–4578.

[18] H. Caesar, V. Bankiti, A. H. Lang, S. Vora, V. E. Liong, Q. Xu, A. Krishnan, Y. Pan, G. Baldan, and O. Beijbom, "nuscenes: A multimodal dataset for autonomous driving," in *Proceedings of the IEEE/CVF conference on computer vision and pattern recognition*, 2020, pp. 11 621–11 631.

[19] M.-F. Chang, J. Lambert, P. Sangkloy, J. Singh, S. Bak, A. Hartnett, D. Wang, P. Carr, S. Lucey, D. Ramanan, *et al.*, "Argoverse: 3d tracking and forecasting with rich maps," in *Proceedings of the IEEE/CVF conference on computer vision and pattern recognition*, 2019, pp. 8748–8757.

[20] B. Wilson, W. Qi, T. Agarwal, J. Lambert, J. Singh, S. Khandelwal, B. Pan, R. Kumar, A. Hartnett, J. K. Pontes, D. Ramanan, P. Carr, and J. Hays, "Argoverse 2: Next generation datasets for self-driving perception and forecasting," in *Proceedings of the Neural Information Processing Systems Track on Datasets and Benchmarks (NeurIPS Datasets and Benchmarks 2021)*, 2021.

[21] Y. Liu, T. Yuan, Y. Wang, Y. Wang, and H. Zhao, "Vectormapnet: End-to-end vectorized hd map learning," in *International Conference on Machine Learning*. PMLR, 2023, pp. 22 352–22 369.

[22] W. Van Gansbeke, B. De Brabandere, D. Neven, M. Proesmans, and L. Van Gool, "End-to-end lane detection through differentiable least-squares fitting," in *Proceedings of the IEEE/CVF International Conference on Computer Vision (ICCV) Workshops*, Oct 2019.

[23] L. Tabelini, R. Berriel, T. M. Paixao, C. Badue, A. F. De Souza, and T. Oliveira-Santos, "Polylanenet: Lane estimation via deep polynomial regression," in *2020 25th International Conference on Pattern Recognition (ICPR)*. IEEE, 2021, pp. 6150–6156.

[24] Z. Zhang, Y. Zhang, X. Ding, F. Jin, and X. Yue, "Online vectorized hd map construction using geometry," in *Computer Vision – ECCV 2024*. Cham: Springer Nature Switzerland, 2025, pp. 73–90.

[25] X. Liu, S. Wang, W. Li, R. Yang, J. Chen, and J. Zhu, "Mgmap: Mask-guided learning for online vectorized hd map construction," in *Proceedings of the IEEE/CVF Conference on Computer Vision and Pattern Recognition (CVPR)*, June 2024, pp. 14 812–14 821.

[26] B. A. Galler and M. J. Fisher, "An improved equivalence algorithm," *Commun. ACM*, vol. 7, no. 5, p. 301–303, May 1964. [Online]. Available: https://doi.org/10.1145/364099.364331